This was installed on 5/7/14.

Appendix M: Why the transverse vector potential $\mathbf{A_t}$ is small for a transmission line

Claim: In the King gauge, the transverse vector potential $\mathbf{A_t}$ may be neglected. (M.1)

The vector potential is written below as $\mathbf{A_t} = \int_{conductors} dxdy\ \mathbf{J_t}(x,y) * (stuff)$.
We shall make the following three claims:

(1) $|\mathbf{J_t}| < 10^{-3}\ |J_z|$ for f = 0 Hz to 1000 GHz (which is to say: "transverse currents are small inside the conductors") *(M.13)*
(2) in the $\mathbf{A_t}$ integral there is a cancellation effect not present in the A_z integral which in effect reduces $\mathbf{A_t}$ by a factor of 10 (ballpark) relative to A_z . *(M.14)*
(3) the net ballpark result is that $|\mathbf{A_t}| < 10^{-4}\ |A_z|$ for f = 0 Hz to 1000 GHz which supports the opening claim (M.1) above. *(M.22)*

According to (1.5.9) one can express the King gauge vector potential at all points in space in terms of the currents in the transmission line conductors in this manner,

$$\mathbf{A}(\mathbf{x},\omega) = \frac{1}{4\pi}\ \Sigma_i \int \mu_i\ \mathbf{J_i}(\mathbf{x}',\omega)\ \frac{e^{-j\beta_d R}}{R}\ dV' \qquad R = |\ \mathbf{x} - \mathbf{x}'\ | \qquad (1.5.9)$$

where Σ_i is a sum over all the conductors, and β_d is the wavenumber in the dielectric. Therefore, the transverse part $\mathbf{A_t}$ may be written as an integral of the transverse conductor currents $\mathbf{J_{t,i}}$:

$$\mathbf{A_t}(\mathbf{x}) = \frac{1}{4\pi}\ \Sigma_i\ \mu_i \int \mathbf{J_{t,i}}(x',y',z')\ \frac{e^{-j\beta_d R}}{R}\ dx'\ dy'\ dz' \quad . \qquad (M.2)$$

Transverse of course refers to the x and y directions, where the conductors are aligned in the z direction. The main current in a transmission line conductor is the longitudinal one J_z . When the above equation is processed in the manner of Chapter 4, and one assumes the transmission line limit, the result is

$$\mathbf{A_t}(\mathbf{x}) = -\frac{1}{4\pi}\ \Sigma_i\ \mu_i \int \mathbf{J_{t,i}}(x',y')\ \ln(s^2)\ dx'\ dy' \quad . \qquad s^2 = (x-x')^2 + (y-y'^2) \qquad (M.3)$$

In this transmission line limit, β_d is small (long wavelength) and $e^{-j\beta_d R} \approx 1$. We assume the standard wave functional form such that $\mathbf{J_{t,i}}(x,y,z) = e^{-j\beta_d z}\ \mathbf{J_{t,i}}(x,y)$ and then again set $e^{-j\beta_d z} \approx 1$ for the contributing portion of the dz' integration and that integration produces $-\ln(s^2)$ as in Ch 4 or (J.10).

Meanwhile, Appendix D computes the **E** fields inside a round conductor for each partial wave m, and here we multiply them each by σ to get the current density components,

Second summary of the E field solutions : $R_{dc} = \frac{1}{\sigma\pi a^2}$ $\beta'^2 = \beta^2 - \beta_d^2$ *(D.2.33)*

$J_z(r,m) = \sigma(1/4)\,\eta_m\, I\, R_{dc}\, (a\beta')\,[\frac{J_m(x)}{J_{m+1}(x_a)} - \frac{J_m(x)}{J_{m-1}(x_a)}]$ a = radius $\eta_m \equiv \frac{N_m}{N_0}$

$J_r(r,m) = \sigma(j/4)\,\eta_m\, I\, R_{dc}\, (a\beta_d)\,[\frac{2mx^{-1}J_m(x)}{J_{m-1}(x_a)} + \frac{J_{m+1}(x)}{J_{m+1}(x_a)} - \frac{J_{m+1}(x)}{J_{m-1}(x_a)}]$ $x = \beta' r$

$J_\theta(r,m) = \sigma(1/4)\,\eta_m\, I\, R_{dc}\, (a\beta_d)\,[-\frac{2mx^{-1}J_m(x)}{J_{m-1}(x_a)} + \frac{J_{m+1}(x)}{J_{m+1}(x_a)} + \frac{J_{m+1}(x)}{J_{m-1}(x_a)}]$ $x_a = \beta' a$

The currents are expressed in terms of a cylindrical coordinate system whose z axis runs down the center of the round conductor. Coefficient η_m is the "moment" of the m^{th} partial wave, and the θ-space currents are given by (D.1.3a),

$$\mathbf{J}(r,\theta) = \sum_{m=-\infty}^{\infty} \mathbf{J}(r,m)\, e^{jm\theta} \quad . \qquad \text{// partial wave expansion} \qquad \text{(M.4)}$$

The moments η_m may be obtained by solving the transmission line "capacitor problem" as outlined elsewhere in this document. One finds potential φ, then **E**, then surface charge n(θ), and finally η_m.

The current components are,

$$\mathbf{J} = J_z\hat{\mathbf{z}} + J_r\hat{\mathbf{r}} + J_\theta\hat{\boldsymbol{\theta}} = J_z\hat{\mathbf{z}} + \mathbf{J}_t \qquad \mathbf{J}_t = J_r\hat{\mathbf{r}} + J_\theta\hat{\boldsymbol{\theta}} \quad . \qquad \text{(M.5)}$$

Rather than study these round wire internal solutions in detail, we make two observations:

Observation (1): The transverse currents J_r and J_θ are very small compared to J_z. (M.6)

Looking at (D.2.33) above one sees that the transverse currents J_r and J_θ are in general *smaller* than the longitudinal current J_z by factor $|\beta_d/\beta'|$. In making this claim we regard the combinations of Bessel functions shown in (D.2.33) as being of the same general scale, which can be confirmed by doing elaborate plots of the various complex function magnitudes.

Consider these relations : (first line is from (1.5.1), (3.3.2) with $\varepsilon' \approx \varepsilon$, and (1.1.29) that $v_d = 1/\sqrt{\mu\varepsilon}$)

$$\beta_d = \beta_{d0}\,[1 - j\,(1/2)\tan_L] \approx \beta_{d0} = (\omega/v_d) = 2\pi/\lambda_d \qquad \text{(M.7)}$$

$$\beta = e^{j3\pi/4}\,(\sqrt{2}/\delta) = [(j-1)/\sqrt{2}\,]\,(\sqrt{2}/\delta) = (j-1)(1/\delta) \quad \delta \equiv \sqrt{2/(\omega\mu\sigma)} \qquad \textit{(2.2.21)} \qquad \text{(M.8)}$$

$$\beta'^2 = \beta^2 - \beta_d^2 \; . \qquad \textit{(D.2.2)} \qquad \text{(M.9)}$$

Using these facts there are several ways to write the ratio $|\beta_d/\beta|$, one of which is this:

$$\Rightarrow \; |\beta_d/\beta| = 2\pi\delta/(\sqrt{2}\,\lambda_d) = \sqrt{2}\,\pi\,(\delta/\lambda_d) \qquad \text{(M.10)}$$

which at least suggests that $|\beta_d/\beta|$ is small since one normally thinks of skin depth δ as being much less than the wavelength of a wave on the transmission line. A more useful expression of the ratio however is the following, where we use fact (1.1.2) that $\varepsilon\mu = 1/v_d^2$,

$$|\beta_d/\beta|^2 = (\omega/v_d)^2\,\delta^2/2 = (\omega/v_d)^2 * 1/(\omega\mu\sigma) = \frac{\omega}{v_d^2\mu\sigma} = \frac{\varepsilon\omega}{v_d^2\varepsilon\mu\sigma} = \frac{\varepsilon\omega}{\sigma}$$

$$\Rightarrow \; |\beta_d/\beta| = \sqrt{\varepsilon\omega/\sigma}\;. \qquad \text{(M.11)}$$

We see that at $\omega = 0$ (DC) this ratio is 0 and it then gradually increases with ω as $\omega^{1/2}$. If we are willing to restrict our transmission line interests to f < 1000 GHz, and if the conductors are copper, we find that the ratio $|\beta_d/\beta|$ will always be less than the following:

$$\sqrt{\varepsilon\omega/\sigma} \approx \sqrt{\varepsilon_0\omega/\sigma} = \sqrt{\varepsilon_0 2\pi f/\sigma} = [8.85 \times 10^{-12} * 2\pi * 10^{12} / 5.81 \times 10^{7}\,]^{1/2} = 10^{-3} \qquad \text{(M.12)}$$

```
evalf(sqrt((8.85e-12*2*Pi*1e12/5.81e7)));
                                .0009783032660
```

Thus, all the way from f = 0 to f = 1000 GHz, we have $|\beta_d/\beta| < 10^{-3}$. At 10 GHz the ratio is 10^{-4}.

Since $|\beta| << |\beta_d|$, it follows that $\beta'^2 = \beta^2 - \beta_d^2 \approx \beta^2$ so then $\beta' = \beta$ for all practical purposes and then we have shown that $|\beta_d/\beta'| << 10^{-3}$. Thus,

$$|J_r| < 10^{-3}\,|J_z|$$
$$|J_\theta| < 10^{-3}\,|J_z| \qquad \text{f = DC to 1000 GHz} \qquad \text{(M.13)}$$

The conclusion then is that the transverse currents are less than 1/1000th of the size of the longitudinal currents for the round copper conductor at all frequencies below 1000 GHz, and we can reasonably assume that a similar conclusion applies to a conductor of any cross sectional shape. This then concludes our "proof" of the claim that "transverse currents are very small" inside the conductors of a transmission line."

Observation (2): In the Helmholtz integration (M.3) there is a large amount of cancellation. (M.14)

Let us consider the nature of this integration in the illustrative case of a two round conductors,

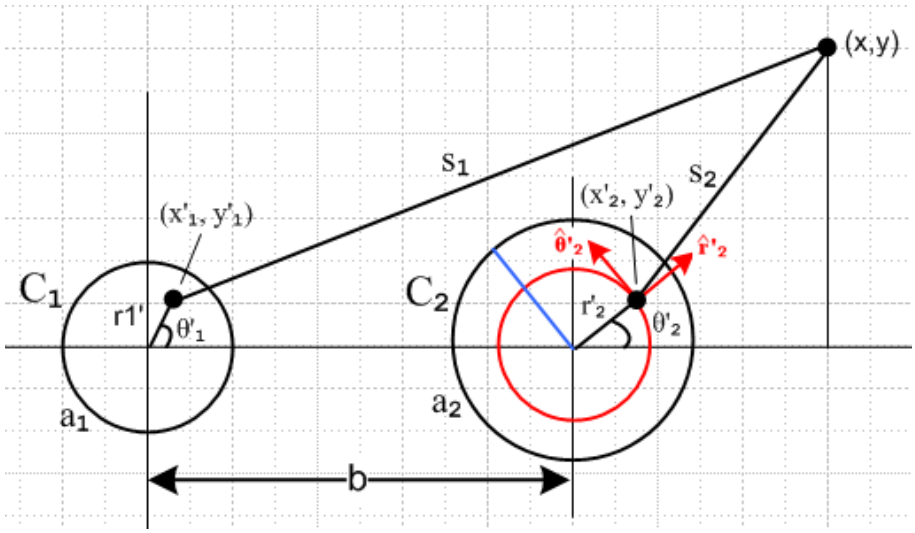


Fig M.1

Consider the contribution to the transverse vector potential component A_x from the right conductor C_2,

$$A_x(x) = -\frac{\mu}{4\pi}\int J_x(x'_2,y'_2)\,\ln(s_2^2)\,dx'_2\,dy'_2 \qquad s_2^2 = (x-x'_2)^2 + (y-y'^2_2) \qquad (M.15)$$

or

$$A_x(x) = -\frac{\mu}{4\pi}\int [J_r(r'_2,\theta'_2)\,\hat{\mathbf{r}}'_2 \bullet \hat{\mathbf{x}} + J_\theta(r'_2,\theta'_2)\,\hat{\boldsymbol{\theta}}'_2 \bullet \hat{\mathbf{x}}]\,\ln(s_2^2)\,[a_2 d\theta'_2]\,dr'_2 \qquad (M.16)$$

or

$$A_x(x) = -\frac{\mu}{4\pi}\int [J_r(r'_2,\theta'_2)\cos\theta'_2 - J_\theta(r'_2,\theta'_2)\sin\theta'_2]\,\ln(s_2^2)\,[a_2 d\theta'_2]\,dr'_2\,. \qquad (M.17)$$

The transverse currents in conductor C_2 have this partial wave expansion from (M.4),

$$J_r(r'_2,\theta'_2) = \sum_{m=-\infty}^{\infty} J_r(r'_2,m)\,e^{jm\theta'_2} \qquad (M.18)$$

and similarly for J_θ . Thus we get

$$A_x(x,y) = -\frac{\mu}{4\pi}a_2\,\Sigma_m\int_0^{a_2} dr'_2\,J_r(r'_2,m)\int_0^{2\pi} d\theta'_2\,e^{jm\theta'_2}\cos\theta'_2\,\ln(s_2^2)$$
$$+\frac{\mu}{4\pi}a_2\,\Sigma_m\int_0^{a_2} dr'_2\,J_\theta(r'_2,m)\int_0^{2\pi} d\theta'_2\,e^{jm\theta'_2}\sin\theta'_2\,\ln(s_2^2) \qquad (M.19)$$

where from (D.2.33) quoted above,

$$J_r(r,m) = \sigma(j/4)\,\eta_m\,I\,R_{dc}\,(a\beta_d)\,\left[\frac{2mx^{-1}J_m(x)}{J_{m-1}(x_a)} + \frac{J_{m+1}(x)}{J_{m+1}(x_a)} - \frac{J_{m+1}(x)}{J_{m-1}(x_a)}\right] \qquad x = \beta' r$$

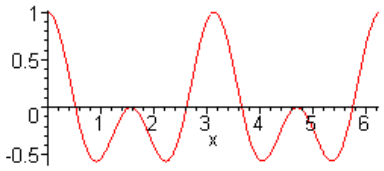
$$J_\theta(r,m) = \sigma(1/4)\,\eta_m\,I\,R_{dc}\,(a\beta_d)\,\left[-\frac{2mx^{-1}J_m(x)}{J_{m-1}(x_a)} + \frac{J_{m+1}(x)}{J_{m+1}(x_a)} + \frac{J_{m+1}(x)}{J_{m-1}(x_a)}\right] \qquad x_a = \beta' a\ .$$

It is in theory possible to first do the $d\theta'_2$ integration in (M.19) and then do the dr'_2 integration and get an analytic result for $A_x(x,y)$. We have dealt with similar angle integrations elsewhere in this document. Rather then attempt this task, we instead consider the portion of the 2D integration represented by the red ring in Fig M.1. On this ring, r'_2 is constant, and our interest is the θ'_2 integration. For any value of m (except for ±1) the trigonometric functions like $e^{jm\theta'_2}\cos\theta'_2$ integrate to 0, for example,

```
f := cos(3*x)*cos(x);
```

$$f := \cos(3x)\cos(x)$$

```
plot(f,x = 0..2*Pi);
```




```
int(f,x = 0..2*Pi);
```

$$0$$

Fig M.2

For these values of m, were it not for the fact that s_2^2 varies around the red circle, $A_x(x,y)$ would be identically 0. Although s_2^2 does vary on the red circle, $\ln(s^2)$ varies very little, and we expect to still have this strong cancellation in the θ'_2 integral so $A_x(x,y)$ is then small. It is true that if $\mathbf{x}$ and $\mathbf{x}'_2$ were to approach the conductor boundary from opposite sides, then $\ln(s^2)$ would vary a lot more and the cancellation would be less, but we ignore this detail in our qualitative argument.

For m = ± 1 this smallness argument fails since for example $\cos^2(\theta'_2)$ does not average to 0 around the red ring. Ignoring the θ'_2 variation in s_2^2 we get in this case (setting $e^{\pm j\theta'_2} \sim \cos\theta'_2$)

$$A_x(x,y) \approx -\frac{\mu}{4\pi} a_2 \sum_m \int_0^{a_2} dr'_2 \; J_x(r'_2,m) \ln(s_2^2) \int_0^{2\pi} d\theta'_2 \cos^2\theta'_2$$

$$\approx -\frac{\mu}{4\pi} a_2 \sum_m \int_0^{a_2} dr'_2 \; J_x(r'_2,\pm 1) \ln(s_2^2)\, \pi \qquad \text{(M.20)}$$

Now we make a different argument which concerns the behavior of the complex Bessel functions as a function of r'_2. As studied in Chapter 2, these functions have a dramatically oscillating phase even in the soft skin depth limit, and we expect then to get cancellation due to this phase as we integrate on the radial segment shown blue in Fig M.1, and again $\ln(s_2^2)$ varies slowly on this ray due to the nature of ln.

The arguments made above for $A_x(x,y)$ also apply to $A_y(x,y)$, and it seems reasonable to assume that the arguments are generally valid for an arbitrary conductor cross section.

Admittedly our analysis here is imprecise and qualitative, but we think it is convincing that there is in fact much cancellation when the transverse currents are integrated over the conductors.

This stands in stark contrast to the longitudinal situation where A_z, being the Helmholtz integral of J_z, involves a generally non-cancelling integration (per conductor) over a generally large current component:

We now wish to compare the following two integrals, where we pick component r to represent a transverse component of $\mathbf{A}_t$,

$$A_{\mathbf{r}}(\mathbf{x}) = -\frac{1}{4\pi} \sum_{\mathbf{i}} \mu_{\mathbf{i}} \int J_{\mathbf{r},\mathbf{i}}(x',y') \ln(s^2)\, dx'\, dy' \quad . \qquad s^2 = (x-x')^2 + (y-y'^2) \qquad \textit{(M.3)}$$

$$A_{\mathbf{z}}(\mathbf{x}) = -\frac{1}{4\pi} \sum_{\mathbf{i}} \mu_{\mathbf{i}} \int J_{\mathbf{z},\mathbf{i}}(x',y') \ln(s^2)\, dx'\, dy' \quad . \qquad s^2 = (x-x')^2 + (y-y'^2) \qquad (M.21)$$

We have shown in (M.13) that $| J_{\mathbf{r}} | < 10^{-3} | J_{\mathbf{z}} |$. Without any mathematical rigor, and allowing a factor of 10 "gain" from the cancellation effect of Observation (2), we make the following *ballpark* estimate,

$$|\mathbf{A}_{\mathbf{t}}| < 10^{-4} |A_{\mathbf{z}}| \qquad f = \text{DC to 1000 GHz.} \qquad (M.22)$$

It is assumed that as ω increases, the transmission line geometry is appropriately shrunk so the transmission line limit remains operative.